



Full Length Article



Growth inhibitory potential of quinone-rich fraction of *Plumbago zeylanica* L. Against MG-63 osteosarcoma cells via Bax/Bcl-2 modulation

Neha Sharma^a, Rasdeep Kour^a, Shagun Verma^a, Vandana Sharma^b, Deepika Singh^b, Sumit G. Gandhi^c, Vaseem Raja^{d,*}, Satwinderjeet Kaur^{a,**}, Naveen Kumar^d, Khalid Mashay Al-Anazi^e, Mohammad Abul Farah^e

^a Department of Botanical & Environmental Sciences, Guru Nanak Dev University, Amritsar 143005, India

^b Quality Management and Instrumentation Division, CSIR- Indian Institute of Integrative Medicine, Canal Road, Jammu 180001, India

^c Infectious Diseases Division, CSIR-Indian Institute of Integrative Medicine, Jammu 180001, India

^d University Center for Research & Development, Chandigarh University, Gharuan, Mohali 140413, Punjab, India

^e Department of Zoology, College of Science, King Saud University, Riyadh 11451, Saudi Arabia

ARTICLE INFO

Keywords:

Cell cycle
Mitochondrial membrane potential
Osteosarcoma
Plumbago zeylanica L.
p53

ABSTRACT

Objective: The objectives of this study were to explore the cytotoxic potential of different fractions (Hexane, chloroform, ethyl acetate and methanol) of *Plumbago zeylanica* L. root powder.

Methodology: In this study, PzMH, PzMC, PzME, and PzMM fractions from the root powder of *P. zeylanica* were obtained through the cold maceration technique. The cytotoxic properties of these fractions on MG-63 cells were assessed using the MTT assay. The most potent fraction was further analyzed to understand its cytotoxic mechanism. To explore its apoptosis-inducing potential, microscopic and flow cytometric studies were conducted. Additionally, western blot analysis was used to examine the expression levels of proteins associated with apoptotic pathways.

Results: PzMH showed the highest cytotoxicity against MG-63 osteosarcoma cells, with a GI₅₀ value of 53.07 µg/ml. Flow cytometric studies revealed an upsurge in reactive oxygen species and disruption of mitochondrial membrane potential. The highest concentration of PzMH fraction (183.48 µg/ml) led to 62 % cell population arrest at G₀/G₁ stage. The anti-apoptotic protein Bcl2 was downregulated, with p53, cleaved-caspase 9, cleaved-caspase3, Bad and Bax expression upregulated. HPLC analysis revealed the presence of lawsone, p-coumaric acid, plumbagin, and 4-hydroxy benzaldehyde, indicating that the quinone-rich fraction of *Plumbago zeylanica* L. attenuates the proliferation of MG-63 osteosarcoma cells through the Bax/Bcl-2 pathway.

Conclusion: To the best of our current knowledge, this marks the first documented case where the hexane fraction enriched with quinones extracted from the roots of *P. zeylanica* demonstrates its ability to induce apoptosis by influencing the Bax/Bcl2 pathway.

1. Introduction

Last few decades have witnessed a tremendous advancement in health care system, still cancer continues to be a major global public health issue and remains one of the leading causes of death worldwide. The rising incidence of cancer is particularly evident in Africa, Asia, and

Central and South America, which together account for more than 70 % of all cancer-related deaths worldwide. (Nguyen et al.,2020). Based on the data from the Global Cancer Observatory, lung cancer emerged as the predominant etiology of cancer related mortality globally in the year 2020 (Chhikara & Parang, 2022). A substantial proportion of lung cancer cases are typically diagnosed at an advanced stage, characterized

Abbreviations: Rh-123, Rhodamine-123; PVDF, Polyvinylidene fluoride; PI, Propidium Iodide; PAGE, Polyacrylamide gel electrophoresis; MG-63, Human Osteosarcoma Cell line; LA, Late apoptosis; FBS, Fetal Bovine Serum; EB, Ethidium bromide; EDTA, Ethylenediaminetetraacetic acid; EA, Early apoptosis; DMSO, Dimethyl Sulfoxide.

* Corresponding author at: University Center for Research & Development, Chandigarh University, Gharuan, Mohali 140413, Punjab, India.

** Corresponding author at: Department of Botanical & Environmental Sciences, Guru Nanak Dev University, Amritsar 143005, India.

E-mail addresses: wrajamp2009@gmail.com (V. Raja), satwinderjeet.botenv@gndu.ac.in (S. Kaur).

<https://doi.org/10.1016/j.jksus.2024.103405>

Received 27 April 2024; Received in revised form 19 August 2024; Accepted 20 August 2024

Available online 22 August 2024

1018-3647/© 2024 The Authors. Published by Elsevier B.V. on behalf of King Saud University. This is an open access article under the CC BY license (<http://creativecommons.org/licenses/by/4.0/>).

by metastatic spread. Notably, bone metastasis gradually manifest in the majority of individuals affected by lung cancer. Compared to the 12 to 15 months of survival typically seen in patients with metastatic lung adenocarcinoma, those with bone metastasis from lung cancer face a grim outlook, with median overall survival ranging between 6 and 8 months. (Chambard et al., 2018). One of the most common malignant primary bone cancers is osteosarcoma (OS), which has a peak frequency either in young people or people older than 50 years. (Rabelo et al., 2022). The 5-year overall survival rate of nonmetastatic OS patients is nearly 77 %, whereas the 5-year overall survival rate of metastatic OS patients is less than 20 %. The possible causes of osteosarcoma can be prior therapeutic radiotherapy, tall height, heavy weight at the time of birth and many pre-existing cancer susceptibility syndromes, such as Li-Fraumeni syndrome, Paget's disease and inherited retinoblastoma (Cole et al., 2022). Due to some biochemical intricacies involved in tumor formation, the specific etiology of bone cancer is still unknown. Cell cycle deregulation and lack of apoptosis are considered essential hallmarks of cancer cells (Koh et al., 2020). Genetic alterations, coupled with dysregulated expression of cell cycle regulators and the loss of tumor suppressor alleles, have been associated with the inactivation of tumor suppression mechanism. This inactivation allows cells to bypass crucial checkpoints and undergo uncontrolled proliferation (Abreu Velez & Howard, 2015).

Malignant diseases frequently present formidable challenges when it comes to their treatment using conventional therapeutic approaches, primarily due to the dual burdens of economic constraints and the debilitating side effects associated with these treatments. Research shows phytochemicals have potential for chemoprevention and chemotherapy (Zhang et al., 2022). Natural plant compounds including capsaicin, Asiatic acid, honokiol, and betulinic acid cause apoptosis by downregulating pro-survival/anti-apoptotic markers like Bcl-2 and Bcl-xl and upregulating pro-apoptotic markers like cytochrome c, bax, and activating the caspase cascade. Similarly, ginsenoside, atractylodin, β -eudesmol, fucosterol, thymol and silymarin arrest cell cycle at G₀/G₁ and G₂/M phases (Koh et al., 2020).

Plumbago zeylanica L. is a well-known herbal plant commonly known as Ceylon leadwort (Tokarz et al., 2020). *P. zeylanica*, a perennial plant, in Ayurveda, is known as chitrak and its roots as chitramula (Bhinde et al., 2020). It is widely spread in India and Sri Lanka and has antioxidant, antimicrobial, anti-inflammatory, antidiabetic, anti-hyperlipidemic, antiulcer and hepatoprotective activities (Shukla et al., 2021). Quinones, divided into naphthoquinones, benzoquinones, and anthraquinones, possess various pharmacological properties, including anticancer, apoptotic, antibiotic, antiallergenic, antiviral, antiplatelet inhibitory, anti-ringworm, antifungal, blood thinning, and radical scavenging properties (Rahman et al., 2022). Therefore, this study focused on exploring the anticancer potential of *P. zeylanica* L. which is rich in quinones against MG-63 osteosarcoma cell line.

2. Materials and methods

2.1. Extract preparation and cell culture

Roots of *Plumbago zeylanica* L. were obtained from Amritsar (Majith Mandi) and authenticated at CSIR-CIMAP in Lucknow, India. The voucher specimen (Accession no. P035) was submitted to the CSIR-CIMAP crude drug repository. The roots were dried and powdered and subsequently macerated in various solvents viz. hexane, chloroform, ethyl acetate and methanol for 72 h, resulting in PzMH (0.17 %), PzMC (0.40 %), PzME (0.58 %) and PzMM (6.25 %) fractions respectively. The extracts were filtered and concentrated using a rotavapor (Buchi R-210, Flawil, Switzerland).

The MG-63 (osteosarcoma) cells were obtained from the National Centre for Cell Science (NCCS) Pune and grown in culture flasks using DMEM medium, to encourage ideal cellular development, media was enhanced with 10 % FBS and treated with sodium bicarbonate. A precise

temperature of 37 °C and 5 % carbon dioxide was maintained in the culture environment.

2.2. Assessment of cytotoxic activity and cell migration assay

The cytotoxic activity of *P. zeylanica* fractions was assessed using an MTT assay with few adjustments (Mickisch et al., 1990). MG-63 cells (8×10^3 cells/well) were seeded in a 96 wells microplate and placed in CO₂ incubator for 24 h. Subsequently different concentrations of *P. zeylanica* root fractions (15.625 to 500 μ g/ml) were used to treat the cells for 24 h. After 48 h, the cells in each well were treated with 20 μ l MTT and incubated for 3 h to assess the capacity of living cells to convert MTT into insoluble formazan crystals (purple colored). The optical density measurements at 570 were carried out with the help of a multi-well plate reader and percent growth inhibition was calculated with the following formula

$$\% \text{Growth Inhibition} = \frac{\text{Abs}_c - \text{Abs}_t}{\text{Abs}_c} \times 100$$

where, Abs_c: absorbance of untreated control cells, Abs_t: absorbance of cells treated with *P. zeylanica* root fractions the method of

Cell migration capability was tested using a cell scratch experiment as per the method of (Liang et al., 2007).

2.3. Morphological changes and nuclear morphology analysis

In a 6-well plate, MG-63 cells (8×10^5 /well) were grown and incubated with various concentrations of PzMH fraction (15.35, 53.07 and 183.48 μ g/ml) for 24 h following confluency. The cells were observed under an inverted microscope and images were acquired (Nikon Eclipse TS2, Tokyo, Japan) to study the nuclear morphology. The PzMH fraction, at concentrations of 15.35, 53.07, and 183.48 μ g/ml, was introduced into the cellular milieu for a duration of 24 h. post-incubation, the cells underwent fixation for 20 min in cold paraformaldehyde (4 %) within a light-restricted environment, followed by a thorough rinse with saline phosphate-buffered (PBS). Subsequent to this step, the cells were subjected to incubation with DAPI dye (10 μ g/ml) for a period of 30 min. Thereafter, alterations in nuclear morphology were meticulously assessed utilizing a fluorescence microscope, with subsequent capture of images for further analysis.

2.4. AO/EtBr parallel staining for apoptosis detection and mitochondrial transmembrane potential using a fluorescence microscope

MG-63 cells, (4×10^5 cells/well), were cultured, in a six-well plate, followed by 24 h treatment with PzMH fraction (15.35, 53.07 and 183.48 μ g/ml). The cells were collected and subjected to a 5-min incubation in a light-restricted environment with a solution containing AO/EtBr (100 μ g/ml) with two dyes combined in equal proportions. To detect, the mitochondrial membrane potential (MMP) changes in osteosarcoma cells treated with PzMH fraction, rhodamine 123 (Rh-123) dye was used. MG-63 osteosarcoma cells were exposed to various fractions of PzMH for 24 h. After treatment, the cells were fixed in 70 % ethanol after a thorough washing with PBS. They were then placed in a carbon dioxide (CO₂) incubator for a duration of 30 min, during which they were exposed to Rh-123 dye (2 μ g/ml). After that, remnants of dye were eliminated by washing the cells with PBS thrice before scanning them with a fluorescence microscope.

2.5. Apoptosis detection and cell cycle analysis using Annexin V-FITC/PI double staining

Apoptosis detection was investigated using Annexin V-FITC kit (Sigma). In a 6-well plate, MG-63 cells were cultured for 24 h and subsequently treated with varying concentrations of PzMH fraction for

24 h. Attached and floating cells were gathered after treatment and centrifuged at 1200g for 5 min and washed twice with PBS. Cells were again centrifuged, at 1200g, resuspended in 0.1 ml binding buffer for 15 min and subsequently treated with 5 μ l Annexin V-FITC conjugate and 5 μ l propidium iodide (PI) for 20 min. The labeled cells were examined using a flow cytometer. The method of Rasul *et al.*, (2011) was used for cell cycle analysis.

2.6. Cell cycle phase distribution analysis and reactive oxygen species generation analysis

The BD cycle DNA kit was employed for the analysis of cell cycle stages. MG-63 cells were subjected to treatment using different amounts of the *PzM*H component. Following a 24 h incubation period, cellular samples were harvested, subjected to centrifugation, and subsequently preserved in a solution of 70 % chilled ethanol. The samples were subjected to fixation using trypsin buffer, followed by incubation at 37 °C for a duration of 5 min. Subsequently, the samples were treated with RNase buffer and trypsin inhibitor. A 200 μ l solution of cold PI stain was added, to the mixture and allowed to cool on ice for a duration of 1 h. The flow cytometer was employed for the analysis of cells that had been labeled.

In a 6-well plates the MG-63 cells were cultured for 24 h, subsequently subjected to a 24 h exposure to the *PzM*H fraction. After treatment, the cells underwent a rinsing process utilizing phosphate-buffered saline (PBS) and then were subjected to a 30-min treatment with DCFH-DA (5 μ g/ml PBS). Following the process of centrifugation, the cells were collected, subjected to another round of centrifugation, and subsequently reconstituted in 500 μ l of PBS. The cells were promptly analyzed utilizing the FL-1 channel of the flow cytometer, with an excitation wavelength of 488 nm and an emission wavelength of 535 nm.

2.7. Mitochondrial membrane potential analysis using flow cytometer, western blot analysis and HPLC of the *PzM*H fraction

In 6-well plates MG-63 osteosarcoma cells were grown for 24 h, and treated with *PzM*H fraction, and then decanted. Rh-123 was added for 30 min. Cells were collected, centrifuged, and resuspended in 500 μ l PBS. The FL-1 channel was used to examine the cells. The cells were then examined using a flow cytometer (O'Connor *et al.*,1988).

For western blotting the MG-63 cells were treated with GI_{30} , GI_{50} and GI_{70} concentrations of *PzM*H fraction for 24 h, and RIPA lysis buffer was used to extract proteins from the cells and separated on a 10 % SDS-PAGE with subsequent transfer to a PVDF membrane. 5 % skimmed milk was used to block the membrane, and then incubated with specific primary antibodies. The membrane was then rinsed twice with saline phosphate buffer and incubated with secondary antibodies. ECL (Enhanced chemiluminescence) plus reagent was used to detect protein bands, and ImageJ software was used for intensity analysis. The ultimate quantification of each protein's expression was determined by dividing its expression level by the expression level of β -actin in the respective sample. High-performance liquid chromatography (HPLC), of *PzM*H fraction was performed as per of Engida *et al.*(2013).

2.8. Statistical analysis

The analysis of the data was carried with the help of IBM SPSS software and represented as mean \pm SE (n = 3). Significant differences between the different groups were calculated with ANOVA with p \leq 0.05 significant level. In addition, the Tukey test was performed to calculate the HSD.

3. Results

*PzM*H, *Pz*MC, *Pz*ME, *Pz*MM obtained from the root powder of *Plumbago zeylanica* L. were investigated for their cytotoxic potential using

MTT assay on MG-63 cell line. *PzM*H fraction exhibited the highest cytotoxic potential amongst all fractions with 53.07 μ g/ml GI_{50} value in MG-63 cells (Table 1). As *PzM*H fraction possessed the highest cytotoxic activity in MG-63 osteosarcoma, further experimentation was performed on this cell line using *PzM*H fraction.

3.1. *PzM*H fraction possessed anti-migratory potential

A scratch migration experiment was employed to investigate the inhibitory activity of the *PzM*H fraction on the migratory behavior of osteosarcoma (MG-63 cells). The measurement of cells migrated was analyzed by using ImageJ software. The pre- and post-treatment phase-contrast images revealed that following a 24 h treatment with *PzM*H fraction, there was a concentration-dependent decrease in the migration of MG-63 cells towards the scratched area. The MG-63 cell population under controlled conditions, showed that almost all of the areas that were subjected to scratching were successfully covered within a time frame of 24 h (Fig. 1).

3.2. Morphological changes and nuclear morphology

*PzM*H fraction treatment caused morphological alterations in MG-63 cells, including detachment, membrane rounding, and blebbing. Control cells exhibited thick multilayers, while *PzM*H treated cells showed rounding off, contact loss, and increased intercellular space (Fig. 2 A). Apoptosis is programmed cell death, and DAPI staining shows healthy nuclei in untreated MG-63 cells, while increased *PzM*H fraction causes fragmentation and shrinkage (Fig. 2 B).

3.3. AO/EtBr parallel staining for apoptosis

*PzM*H fraction treatment led to increased apoptosis in cells compared to control cells. Cells treated with varying concentrations of *PzM*H fraction displayed apoptosis-like characteristics. Early apoptosis was observed in cells treated with GI_{30} (15.35 μ g/ml), while late apoptosis was observed in cells treated with GI_{50} (53.07 μ g/ml). Most cells experienced apoptosis at GI_{70} (183.48 μ g/ml), indicating increased apoptotic or necrotic cells (Fig. 2 C).

Table 1
Percent growth inhibitory activity of *P. zeylanica* fractions against MG-63 cells.

MG-63				
Concentration (μ g/ml)	<i>PzM</i> H	<i>Pz</i> MC	<i>Pz</i> ME	<i>Pz</i> MM
15.625	27.01 \pm 0.76 ^d	20.74 \pm 1.08 ^d	15.60 \pm 0.97 ^c	12.66 \pm 2.11 ^c
31.25	44.06 \pm 2.48 ^c	27.71 \pm 2.28 ^d	22.84 \pm 2.4 ^{de}	21.69 \pm 1.56 ^d
62.5	54.79 \pm 2.38 ^b	41.69 \pm 2.05 ^c	24.26 \pm 1.38 ^d	28.05 \pm 0.91 ^{cd}
125	62.98 \pm 1.96 ^b	51.09 \pm 1.59 ^b	33.33 \pm 0.89 ^c	34.08 \pm 2.78 ^{bc}
250	76.18 \pm 1.20 ^a	58.41 \pm 1.11 ^b	51.06 \pm 1.83 ^b	42.98 \pm 1.32 ^b
500	84.33 \pm 2.23 ^a	73.47 \pm 2.05 ^a	65.62 \pm 2.00 ^a	56.68 \pm 2.07 ^a
GI_{50}	53.07 μ g/ml	119.00 μ g/ml	246.72 μ g/ml	376.12 μ g/ml
R ²	0.9875	0.9899	0.9196	0.9791
F Ratio	117.29*	124.62*	131.43*	68.51*
Regression Equation	y = 16.124ln(x) - 14.04	y = 15.05ln(x) - 21.927	y = 14.172ln(x) - 28.063	y = 11.954ln(x) - 20.886
HSD	0.09	0.082	0.078	0.09

(*p \leq 0.05). The values are given as mean \pm SE. Data labels with different letters in a column indicate a significant difference between the.

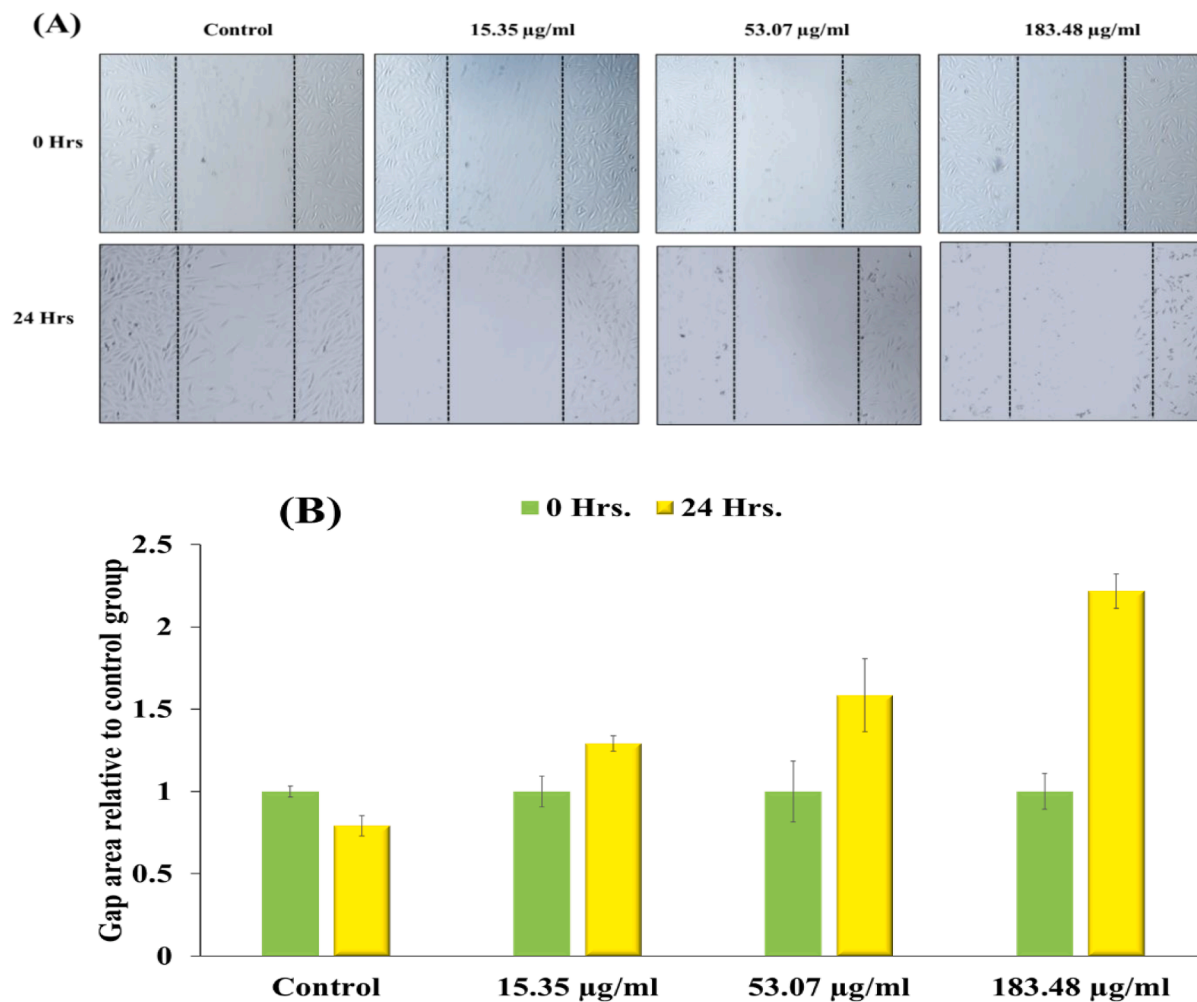


Fig. 1. (A) *PzMH* fraction inhibited the migration of MG-63 cells. (B) Representative bar graph showing quantitative analysis of cell migration.

3.4. Mitochondrial membrane potential assessment

Depolarization of mitochondrial membrane was studied using Rh-123 dye. *PzMH* administration at a 15.35 µg/ml concentration significantly promoted depolarization. *PzMH* fractions treated with 183.48 µg/ml showed higher depolarization compared to those treated with 53.07 µg/ml (Fig. 2 D).

3.5. *PzMH* fraction induces apoptosis and cell cycle arrest at sub-G1 stage

The *PzMH* fraction increased late and early apoptotic cells in treated cells compared to untreated cells. An increase of about 21.2 % in early apoptotic (EA) cells was observed at 15.35 µg/ml concentration, while a small increase of about 7.6 % was also observed in control cells. At 53.07 µg/ml, early apoptotic cells increased by (56.5 %), while late apoptotic cells increased by (7.7 %). At 183.48 µg/ml, 73.8 % of cells were in the EA stage. *PzMH* fraction induces apoptosis in a concentration-dependent manner and inhibits osteosarcoma cell proliferation (Fig. 3A&B). *PzMH* fraction treatment at different concentrations led to sub-diploid cell accumulation in the sub-G₁ phase, stopping cell cycle progression. MG-63 cells exposed to *PzMH* fraction for 24 h showed arrest rates of 59.2 %, 70.6 % and 83.5 % at the sub-G₁ stage at 15.35, 53.07, and 183.48 µg/ml concentrations, respectively (Fig. 3 C&D).

3.6. Analysis of cell cycle phase distribution and effect on reactive oxygen species (ROS)

PzMH fraction treatment resulted in the arrest of 62 % of cells in the G₀/G₁ phase at the maximum tested dose of 183.48 µg/ml whereas, untreated control cells showed 20.9 % cells in this stage. At the G₀/G₁ stage, the GI₅₀ concentration (53.07 µg/ml) produced 46.1 % cell population arrest. The lowest concentration (15.35 µg/ml) caused 39.6 % G₀/G₁ phase cell cycle arrest (Fig. 4 A&B). The generation of ROS in the *PzMH* treated cells increased by 38 %, 53.5 %, and 76.2 % respectively, while the population of intact cells decreased by 62 %, 46.5 %, and 23.8 % respectively, compared to untreated cells which had a ROS generation of 26.4 % and intact cell population of 73.6 % (Fig. 4 C&D).

3.7. *PzMH* fraction influence on mitochondrial membrane potential (MMP; Δψ_m) and western blotting

PzMH (15.35, 53.07 and 183.48 µg/ml) fraction treated MG-63 cells showed a 46.1 %, 55.7 %, and 80.4 % reduction in mitochondrial membrane integrity respectively as compared to control cells. The presence of intact mitochondria was revealed by increased dye accumulation. However, increased *PzMH* fraction lost mitochondrial integrity, and dye fluorescence. The membrane potential of MG-63 cells was attenuated in a concentration-dependent manner after 24 h (Fig. 5A&B). *PzMH* treated MG-63 cells showed increased p53, Bax, Bad, cleaved-caspase 3, and cleaved-caspase 9 protein expression, while Bcl-2 expression was reduced. Upregulated cleaved-caspase 3 expression

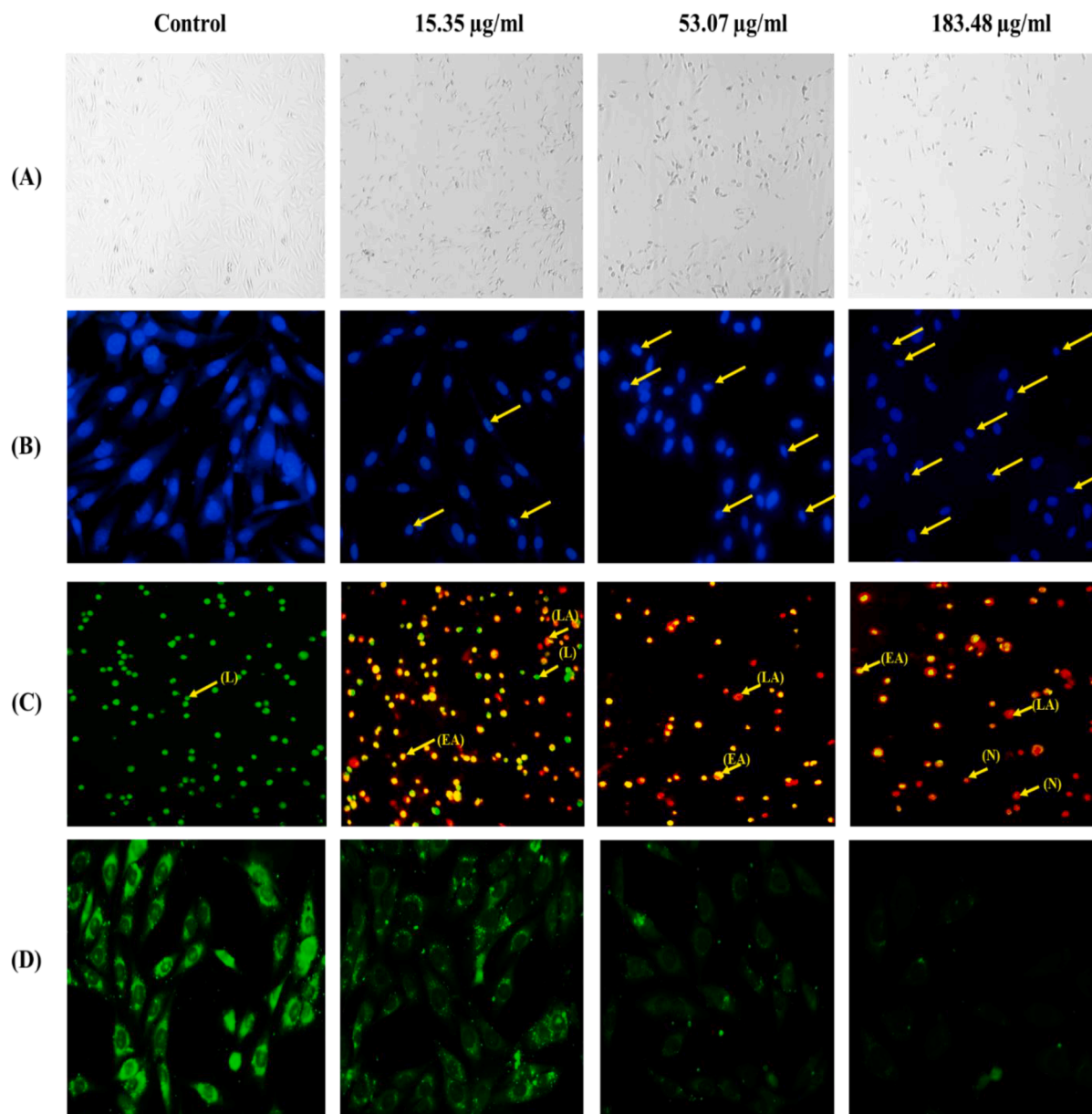


Fig. 2. Photomicrographs of untreated control and *PzMH* fraction treated MG-63 cells for 24 h (A) Phase contrast micrography. (B) Staining with DAPI. Arrows indicate changes in nuclear morphology. (C) AO/EtBr double staining. (D) Micrographs of untreated and *PzMH* treated MG-63 cells stained with Rhodamine-123.

confirmed intrinsic apoptotic pathway stimulation. The expression level was quantified using the Image J software, and relative expression is presented in the bar graph (Fig. 5 C&D). As a housekeeping protein, β -Actin was used.

3.8. High performance liquid chromatographic (HPLC) analysis of *PzMH* fraction and mechanism of *P. zeylanica* (*PzMH*)-induced cell death in MG-63 cells

HPLC analysis demonstrated the presence of polyphenolic compounds such as, p-coumaric acid retention time (RT), 24.276 min., 4-hydroxybenzaldehyde (RT, 25.676 min), lawsone (RT, 36.132 min) and plumbagin (RT, 47.542 min) (Fig. 6.). Lawsone was found to be in highest quantity (67.154 mg/L) followed by p-coumaric acid (22.746 mg/L), plumbagin (16.623 mg/L) and 4-hydroxybenzaldehyde (6.257 mg/L).

4. Discussion

Medicinal plants contain bioactive substances that can treat and prevent various ailments, including cancer (Roy et al.,2017). Conventional treatments like chemotherapy and radiation therapy have side effects like hair loss, appetite loss, depression, anxiety, and fever (Jain et al.,2016). Research into cytotoxic properties of phyto-therapeutics in cancer treatment has gained attention, with the quinone rich hexane fraction (*PzMH*) exhibiting the highest cytotoxicity against MG-63 cells.

HPLC analysis revealed presence of three, 1,4-naphthoquinones, lawsone and plumbagin in *PzMH* fraction. Naphthoquinones with two carbonyl groups possess the ability to form radical anion or di-anion species by accepting one or two electrons, is what contributes to the various biological activities. Moreover, the electrophilicity of the naphthoquinone ring is reduced by the presence of hydroxy groups at positions 5 and 8 (Kishore et al.,2014). Lawsone is used as the primary precursor in the synthesis of a diverse array of clinically significant anticancer pharmaceuticals, including Atovaquone, Lapachol, and

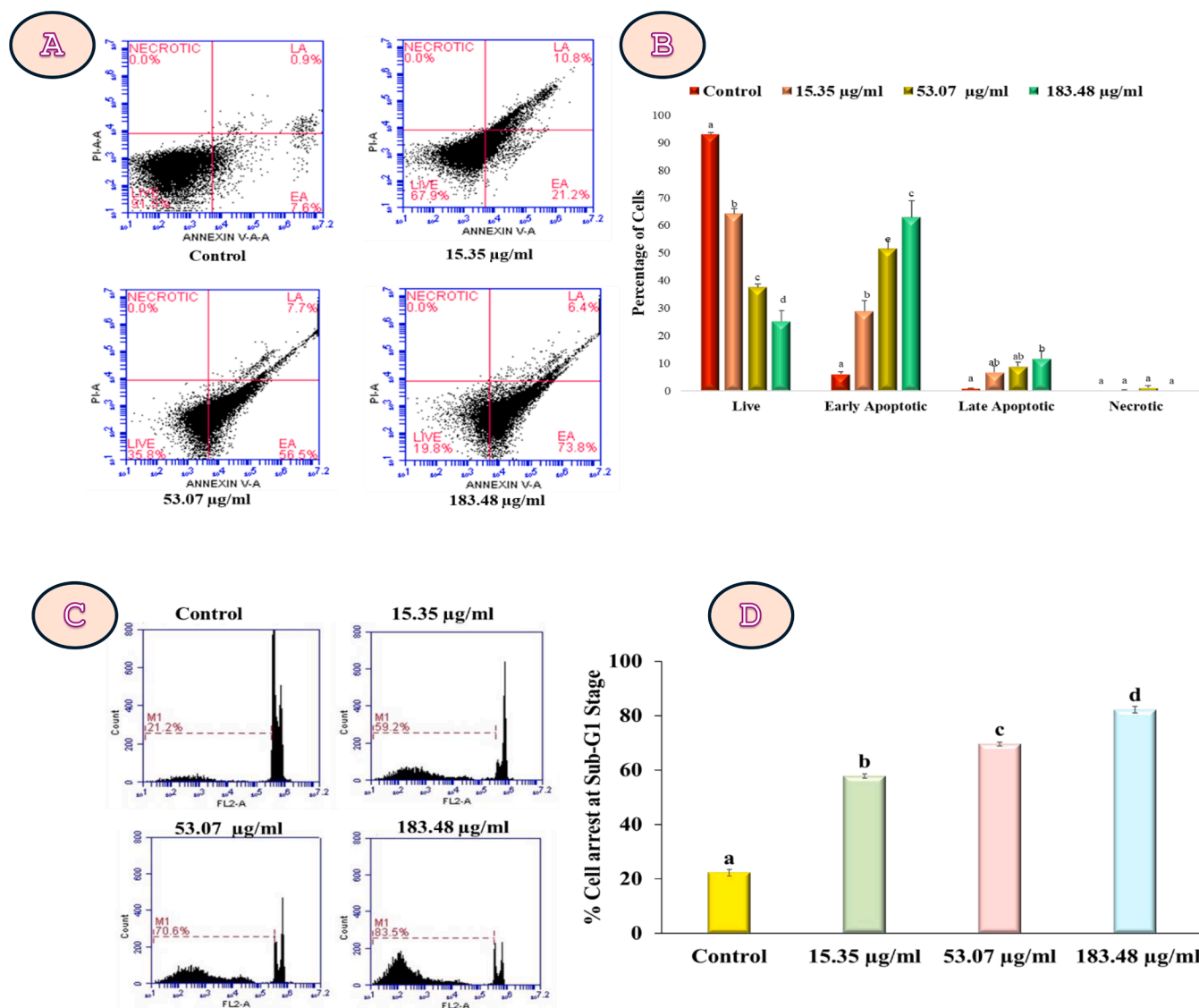


Fig. 3. (A) *PzMH* induced apoptosis in MG-63 cells (B) Histogram representing cell percentage at different stages in control and *PzMH* treated MG-63 cells. (C) represents arrest of cell cycle in at sub-G1 in MG-63 cells by *PzMH* fraction (D) Bar graph represents % cell cycle arrest by *PzMH* fraction at different concentrations.

Dichloroallyl lawsone (Pradhan et al., 2012). Lawsone, when used either independently or in conjunction with cisplatin, effectively curtailed the growth of SKOV-3 cells in a trend contingent on the administered dosage. This treatment hindered SKOV-3 cell growth by halting progression through the G₁/G₀ phase within the cellular life cycle. This arrest was accompanied by an elevation in the expression of p53 and Cip1/p21, which in turn, led to a reduction in the levels of two pivotal proteins, cyclin E and cyclin D1. Furthermore, lawsone was observed to trigger apoptosis by downregulating Bcl-2, enhancing the Bax:Bcl-2 ratio, and activating caspase 3 (Li et al., 2017). Quinone rich *PzMH* fraction inhibit the cell proliferation in MG-63 with the GI₅₀ value of 53.07 µg/ml. The migration of cancer cells to nearby tissues and infiltration into the bloodstream is the cornerstone of the metastatic cascade (Novikov et al., 2021). Osteosarcoma is a kind of bone cancer that is highly aggressive and has a high proclivity for metastasis (Zhu et al., 2021). MG-63 cells subjected to various concentrations of *PzMH* in the cell migration experiment showed a concentration-dependent reduction in cell migration as compared to untreated cells, confirming the anti-migratory potential. Nimlamool et al., (2022) reported similar results wherein a methanolic extract of *Mitrephora chulabhornian* was found to possess anti-proliferative and anti-migratory activity against

HeLa cells (Nimlamool et al., 2022). Natural quinones, plumbagin, juglone, and thymoquinone were shown to effectively suppress the proliferation and migration of PANC-1 cells (Narayanan et al., 2022). MG-63 cell shape changed after they were exposed to varying amounts of *PzMH* fraction. These alterations were marked by cell shortening, loss of membrane integrity and cell shape by becoming fusiform and spherical, eventually detaching from the culture flask, leading to cell death. The morphologic alterations were accompanied by decreased adhesion to the cell culture plates.

The study conducted by Wan et al. (2016) yielded similar results when examining the effects of an ethyl acetate extract derived from *Potentilla chinensis* on MG-63 cells (Wan et al., 2016). Furthermore, DAPI nuclear staining showed signs of apoptosis marked by alterations in nuclear morphology, such as shrinkage of a nucleus, chromatin fragmentation and condensation (Yang et al., 2009). Prior work on MG-63 cells treated with *Sterculia foetida* seed powder extract supports these findings (Jafri et al., 2019).

Additionally, the ability of the *PzMH* fraction to induce apoptosis was evaluated using AO/EtBr double staining under fluorescent microscope and Annexin V-FITC/PI double labeling using flow cytometry. MG-63 cells labelled with AO/EtBr dye and treated with *PzMH* fraction

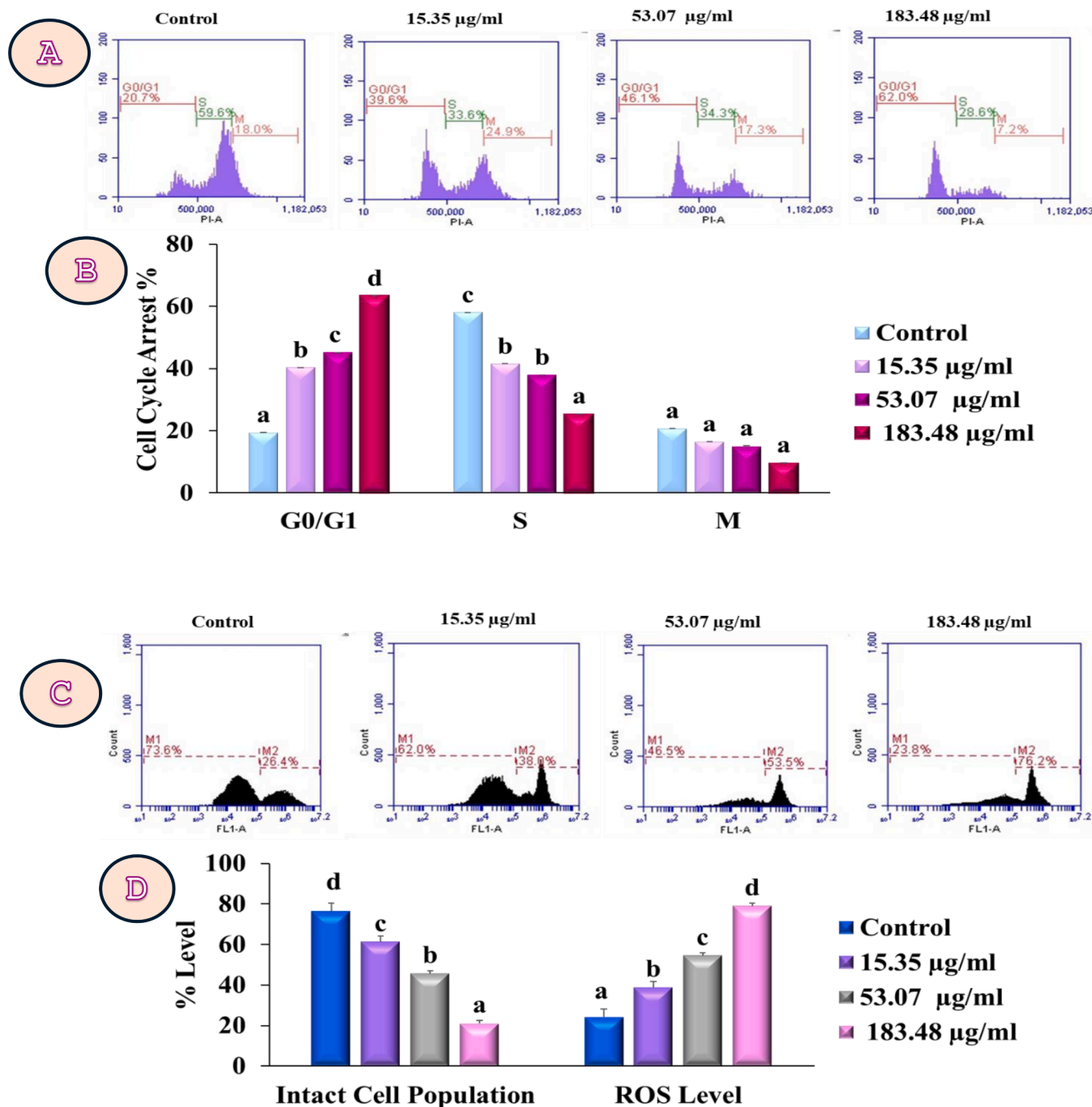


Fig. 4. (A) Represents arrest of cell cycle at G0 /G1 stage by PzMH fraction (B) Bar graph represents cell cycle arrest at different stages in PzMH treated MG-63 cells. (C) PzMH fraction generated concentration dependent ROS in MG-63 cell lines. (D) Percentages of ROS that accumulated in MG-63 cell lines treated with PzMH fraction and untreated control cells are shown in the bar graph.

demonstrated early and late apoptosis in cells treated at higher concentrations. Flow cytometric investigations confirmed these findings, revealing that 73.8 % of cells were in the early stages of apoptosis at 183.48 µg/ml. Ethanolic extract of *Crocus sativus* tepals was reported to suppress the proliferation and migration of U87 glioblastoma cells (Baba et al.,2022). 183.48 µg/ml concentration of PzMH fraction caused an arrest of 62 % cell population at G0/G1 stage. Our results align with Rasouliyan et al., (2021), who demonstrated that lawsone in A549 cells induced apoptosis and caused an arrest in cell cycle at G0/G1 stage (Rasouliyan et al.,2021).

The significance of ROS in cancer is critical. Proliferation of cells, progression of cell cycle, growth and death of cells, cell–cell attachment,

cell migration, blood vessel development and tumor pluripotency maintenance are influenced by ROS (Liou & Storz, 2010). The ROS generation can trigger the permeability of mitochondrial membrane, resulting in MMP loss and membrane integrity (Ma et al.,2014). Flow cytometric investigations revealed that PzMH fraction treated MG-63 cells showed rise in ROS and MMP disruption dose-dependently. Fluorescent imaging of MG-63 cells using the Rh-123 dye produced results consistent with the flow cytometric studies. Cajanol, from *Cajanus cajan*, induced apoptosis via ROS generation and MMP disruption (Luo et al.,2010). Ishteyaqa et al. (2020), showed that a lawsone rich extract of *Lawsonia inermis* killed cancer cells through apoptosis, ROS generation, and interfering with mitochondrial membrane potential

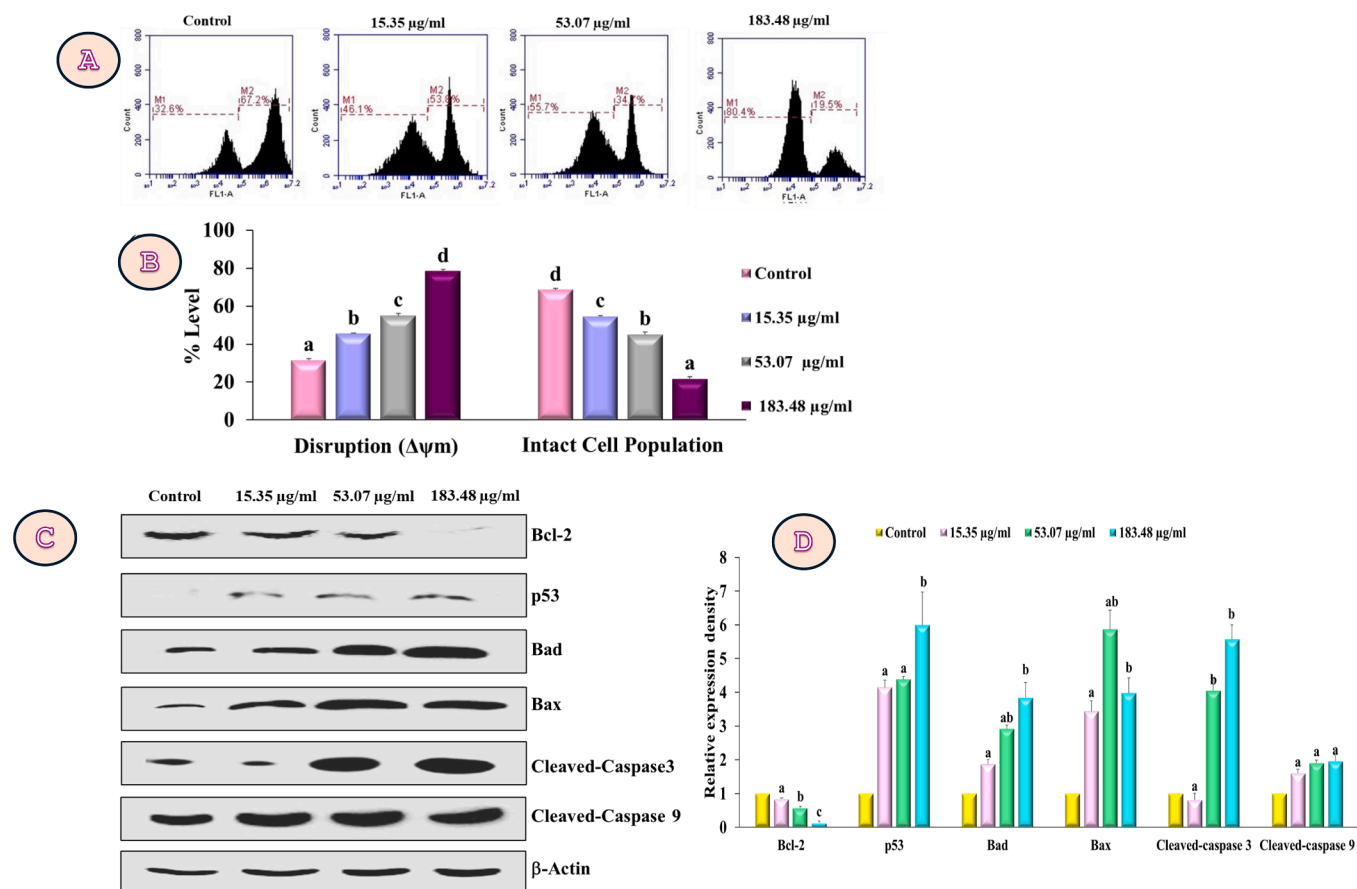


Fig. 5. Rhodamine-123 labeling of MG-63 cells revealed the breakdown of mitochondrial membrane potential ($\Delta\Psi_m$). Bar graph represents % mitochondrial membrane disruption with increase in *PzMH* concentration. (C) Western blot and (D) Represents the transcriptional expression of proteins like Bcl-2, p-53, Bad, Bax, cleaved-caspase3, and cleaved-caspase 9.

(Ishteyaque et al.,2020).

The p53 gene governs apoptosis, senescence, genetic stability, DNA repair and arrest of cell cycle. It also directly participates in the intrinsic apoptosis cascade by increasing outer mitochondrial membrane permeability through its interaction with multidomain Bcl-2 family proteins (Vaseva & Moll, 2009). The interaction between antiapoptotic (Bcl-2) and apoptosis promoting (Bad, Bax) proteins is a hallmark of p53-mediated apoptosis through intrinsic pathway. These molecules act as molecular switches to regulate apoptosis and are found in the outer mitochondrial membrane. Disruption of mitochondrial membrane potential promotes the release of cytochrome c in cytosol, which in turn activates caspase 3 and 9 and trigger the intrinsic apoptotic cascade (Zhou et al.,2019). In the present investigation as *PzMH* fraction treated MG-63 cells displayed upregulation of p53, Bad, Bax, caspase 3 and 9, while a significant decrease in expression of Bcl-2 protein was observed in comparison to control cells. Plumbagin from *Nepenthes alata* increased the Bax/Bcl2 ratio and produced intracellular ROS in MCF-7 cells, resulting in apoptosis (De Laet et al.,2019). The study by Yan et al. (2020), demonstrated that colchicine treatment in Caski and HeLa cells upregulated the expression levels of caspase-3, Bax and cytochrome proteins, while downregulating Bcl-2 protein expression. The outcomes of our investigation demonstrate that the *PzMH* fraction extracted from *P. zeylanica* manifests anticancer properties in MG-63 cells by instigating the activation of the p53-dependent intrinsic apoptotic pathway. This mechanism entails the disruption of the mitochondrial membrane potential ($\Delta\Psi_m$), accumulation of ROS, arrest of cell cycle at G_0/G_1 phase, downregulation in the expression of Bcl-2, and upregulation in the protein expression of p53, Bax, Bad, cleaved-caspase-3 and caspase-9. These impacts are likely attributable to the presence of quinones

within the *PzMH* fraction (Fig. 6).

5. Conclusions

In the current investigation, it was demonstrated that the *PzMH* fraction derived from *P. zeylanica* had significant anti-proliferative effects against MG-63 osteosarcoma cell lines in human. The loss of mitochondrial membrane permeability, subsequent formation of ROS, and arrest of cell cycle at the G_0/G_1 stage initiated the intrinsic mitochondrial-mediated apoptotic pathway in MG-63 cells. The fraction of *Plumbago zeylanica* (*PzMH*) was found to exhibit inhibitory effects on migration and induced apoptosis by upregulating the expression levels of proteins like p53, bad, bax, cleaved-caspases 3 and 9, while downregulating Bcl-2 expression. These findings suggest a significant potential for *PzMH* as an anticancer agent, particularly in the treatment of osteosarcoma. However, further investigation is necessary to fully understand its efficacy and safety profile, ultimately leading to its potential development as a chemotherapeutic drug.

Ethical approval

Not applicable as no animals or humans were involved in this study.

Consent to participate

All authors consent to participate in the publication of the manuscript.

Consent for publication

All authors approve the manuscript to be published.

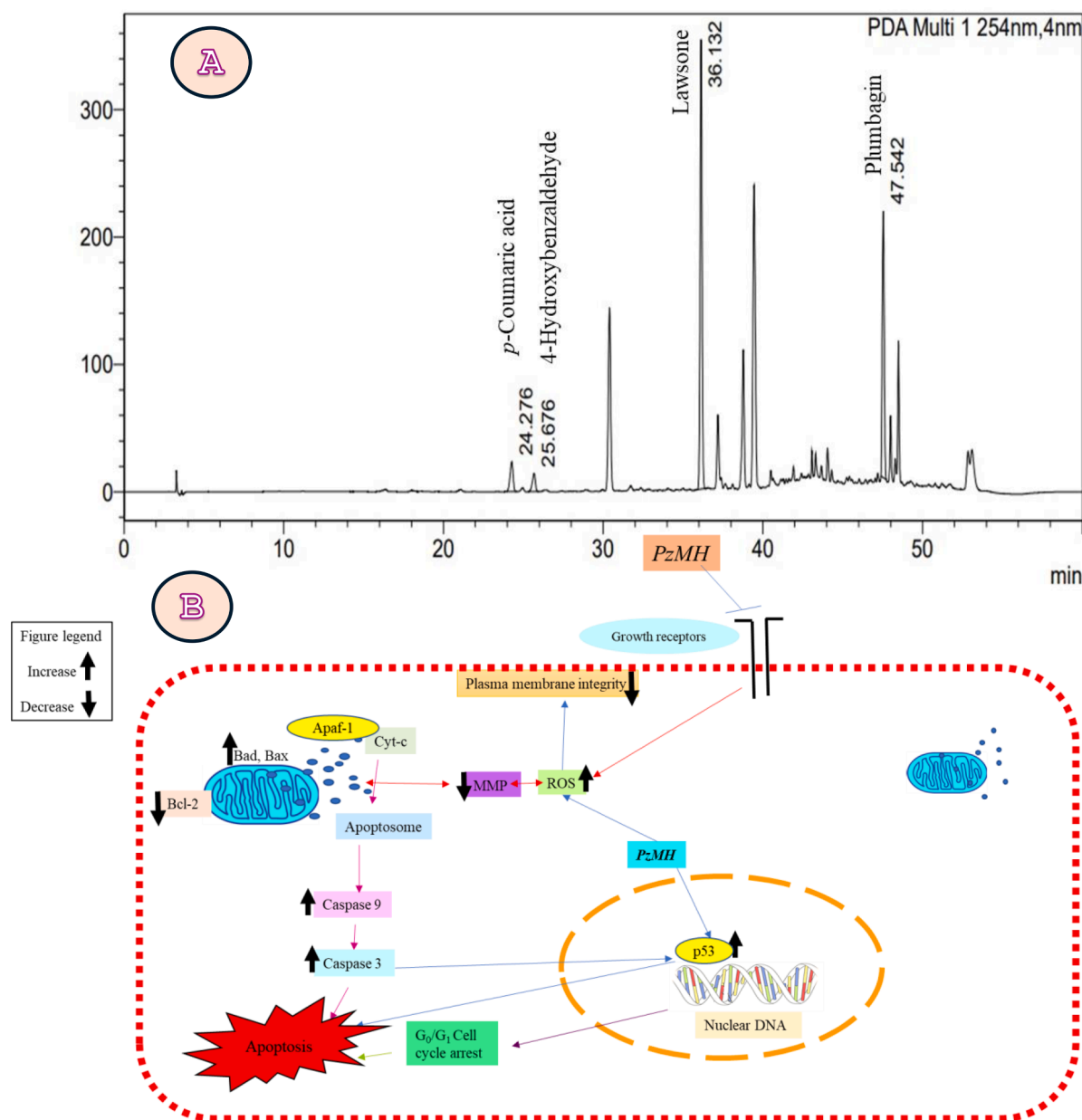


Fig. 6. (A) HPLC chromatogram of PzMH fraction, (B) mechanism of *P. zeylanica* (PzMH)-induced cell death in MG-63 cells.

Funding

Not Applicable.

CRediT authorship contribution statement

Neha Sharma: Writing – original draft, Formal analysis. **Rasdeep Kour:** Methodology, Investigation, Formal analysis. **Shagun Verma:** Methodology, Investigation, Formal analysis. **Vandana Sharma:** Methodology, Data curation. **Deepika Singh:** Methodology, Investigation. **Sumit G. Gandhi:** Writing – review & editing, Supervision, Software, Data curation. **Vaseem Raja:** Writing – review & editing, Writing – original draft, Validation, Conceptualization. **Satwinderjeet Kaur:** Writing – review & editing, Visualization, Validation, Supervision, Project administration, Conceptualization. **Naveen Kumar:** Methodology, Investigation. **Khalid Mashay Al-Anazi:** Writing – review & editing, Resources, Funding acquisition. **Mohammad Abul Farah:** Writing – review & editing, Resources, Funding acquisition.

Declaration of competing interest

The authors declare that they have no known competing financial interests or personal relationships that could have appeared to influence the work reported in this paper.

Acknowledgments

The invaluable support and resources from the CELS and GNDU, Amritsar, India are highly acknowledged. We also extend their heartfelt thanks to Department of Science and technology for their support through DST-FIST and DST-PURSE. The authors would also like to acknowledge King Saud University in Riyadh, Saudi Arabia, for its invaluable support to this research through Project Number (RSP2024R154).

References

- Abreu Velez, A.M., Howard, M.S., 2015. Tumor-suppressor genes, cell cycle regulatory checkpoints, and the skin. *N. Am. J. Med. Sci.* 7 (5), 176–188. <https://doi.org/10.4103/1947-2714.157476>.
- Baba, S.A., Vahedi, M., Ahmad, I., Rajab, B.S., Babalghith, A.O., Irfan, S., Hossain, M.J., 2022. Crocus sativus L. Tepal extract induces apoptosis in human U87 glioblastoma cells. *Biomed Res. Int.*, 4740246 <https://doi.org/10.1155/2022/4740246>.
- Bhinde, S.S., Ravi, A.K., Patgiri, B.J., Harisha, C.R., Shukla, V.J., 2020. Standard operating procedure of Purification of Chitraka (*Plumbago zeylanica* Linn.) along with pharmacognostical and analytical profiles of Plumbagin. *Ayu* 41 (2), 117–122. <https://doi.org/10.4103/ayu.AYU.299.20>.
- Chambard, L., Girard, N., Ollier, E., Rousseau, J.-C., Duboeuf, F., Carlier, M.-C., Brevet, M., Szulc, P., Pialat, J.-B., Wegrzyn, J., Clezardin, P., Confavreux, C.B., 2018. Bone, muscle, and metabolic parameters predict survival in patients with synchronous bone metastases from lung cancers. *Bone* 108, 202–209. <https://doi.org/10.1016/j.bone.2018.01.004>.
- Chhikara, B., Parang, K., 2022. Global cancer statistics 2022: the trends projection analysis. *Chemical Biology Lett.* 10, 451.
- Cole, S., Gianferante, D.M., Zhu, B., Mirabello, L., 2022. Osteosarcoma: a surveillance, epidemiology, and end results program-based analysis from 1975 to 2017. *Cancer*.
- De Laet, C., Matringe, T., Petit, E., Grison, C., 2019. *Eichhornia crassipes*: a powerful bio-indicator for water pollution by emerging pollutants. *Sci. Rep.* 9 (1), 7326. <https://doi.org/10.1038/s41598-019-43769-4>.
- Engida, A.M., Kasim, N.S., Tsigie, Y.A., Ismadji, S., Huynh, L.H., Ju, Y.-H., 2013. Extraction, identification and quantitative HPLC analysis of flavonoids from sarang semut (*Myrmecodia pendan*). *Ind. Crop. Prod.* 41, 392–396. <https://doi.org/10.1016/j.indcrop.2012.04.043>.
- Isheteyaque, S., Mishra, A., Mohapatra, S., Singh, A., Bhatta, R.S., Tadigoppula, N., Mugale, M.N., 2020. In vitro: cytotoxicity, apoptosis and ameliorative potential of *Lawsonia inermis* extract in human lung, colon and liver cancer cell line. *Cancer Invest.* 38 (8–9), 476–485. <https://doi.org/10.1080/07357907.2020.1811300>.
- Jafri, A., Bano, S., Rais, J., Khan, F., Shivanth, N., Sharma, A., Arshad, M., 2019. Phytochemical screening of *Sterculia foetida* seed extract for anti-oxidant, anti-microbial activity, and detection of apoptosis through reactive oxygen species (ROS) generation, mitochondrial membrane potential (MMP) decrease, and nuclear fragmentation in human osteosarcoma cells. *J. Histotechnol.* 42 (2), 68–79. <https://doi.org/10.1080/01478885.2019.1592832>.
- Jain, S., Dwivedi, J., Jain, P.K., Satpathy, S., Patra, A., 2016. Medicinal plants for treatment of cancer: a brief review. *Pharmacognosy J.* 8 (2), 87–102. <https://doi.org/10.5530/pj.2016.2.1>.
- Kishore, N., Binneman, B., Mahapatra, A., van de Venter, M., du Plessis-Stoman, D., Boukes, G., Houghton, P., Marion Meyer, J.J., Lall, N., 2014. Cytotoxicity of synthesized 1,4-naphthoquinone analogues on selected human cancer cell lines. *Bioorg. Med. Chem.* 22 (17), 5013–5019. <https://doi.org/10.1016/j.bmc.2014.06.013>.
- Koh, Y.-C., Ho, C.-T., Pan, M.-H., 2020. Recent advances in cancer chemoprevention with phytochemicals. *J. Food Drug Anal.* 28 (1), 14–37. <https://doi.org/10.1016/j.jfda.2019.11.001>.
- Li, P., Xin, H., Liu, W., 2017. Lawsone inhibits cell growth and improves the efficacy of cisplatin in SKOV-3 ovarian cancer cell lines. *Afr. J. Tradit. Complement. Altern. Med.* 14 (5), 8–17.
- Liang, C.-C., Park, A.Y., Guan, J.-L., 2007. In vitro scratch assay: a convenient and inexpensive method for analysis of cell migration in vitro. *Nat. Protoc.* 2 (2), 329–333. <https://doi.org/10.1038/nprot.2007.30>.
- Liou, G.-Y., Storz, P., 2010. Reactive oxygen species in cancer. *Free Radic. Res.* 44 (5), 479–496. <https://doi.org/10.3109/10715761003667554>.
- Luo, M., Liu, X., Zu, Y., Fu, Y., Zhang, S., Yao, L., Efferth, T., 2010. Cajanol, a novel anticancer agent from *Pigeonpea* [*Cajanus cajan* (L.) Millsp.] roots, induces apoptosis in human breast cancer cells through a ROS-mediated mitochondrial pathway. *Chem. Biol. Interact.* 188 (1), 151–160. <https://doi.org/10.1016/j.cbi.2010.07.009>.
- Ma, C., Wang, Z.Q., Zhang, L.T., Sun, M.M., Lin, T.B., 2014. Photosynthetic responses of wheat (*Triticum aestivum* L.) to combined effects of drought and exogenous methyl jasmonate. *Photosynthetica* 52 (3), 377–385. <https://doi.org/10.1007/s11099-014-0041-x>.
- Mickisch, G., Fajta, S., Keilhauer, G., Schlick, E., Tschada, R., Alken, P., 1990. Chemosensitivity testing of primary human renal cell carcinoma by a tetrazolium based microculture assay (MTT). *Urol. Res.* 18 (2), 131–136. <https://doi.org/10.1007/BF00302474>.
- Narayanan, P., Farghadani, R., Nyamathulla, S., Rajarajeswaran, J., Thirugnanasampandan, R., Bhuwaneswari, G., 2022. Natural quinones induce ROS-mediated apoptosis and inhibit cell migration in PANC-1 human pancreatic cancer cell line. *J. Biochem. Mol. Toxicol.* 36 (5) <https://doi.org/10.1002/jbt.23008>.
- Nguyen, N.H., Ta, Q.T.H., Pham, Q.T., Luong, T.N.H., Phung, V.T., Duong, T.-H., Vo, V. G., 2020. Anticancer activity of novel plant extracts and compounds from *Adenosma bracteosum* (Bonati) in human lung and liver cancer cells. *Molecules* 25 (12), 2912.
- Nimlamool, W., Chansakaow, S., Potikanond, S., Wikan, N., Hankittichai, P., Ruttanapattanakul, J., Thaklaewphan, P., 2022. The leaf extract of *Mitrophora chulabhorniana* suppresses migration and invasion and induces human cervical cancer cell apoptosis through caspase-dependent pathway. *Biomed Res. Int.*, 2028082 <https://doi.org/10.1155/2022/2028082>.
- Novikov, N.M., Zolotaryova, S.Y., Gautreau, A.M., Denisov, E.V., 2021. Mutational drivers of cancer cell migration and invasion. *Br. J. Cancer* 124 (1), 102–114. <https://doi.org/10.1038/s41416-020-01149-0>.
- O'Connor, J.E., Vargas, J.L., Kimler, B.F., Hernandez-Yago, J., Grisolia, S., 1988. Use of rhodamine 123 to investigate alterations in mitochondrial activity in isolated mouse liver mitochondria. *Biochem. Biophys. Res. Commun.* 151 (1), 568–573. [https://doi.org/10.1016/0006-291x\(88\)90632-8](https://doi.org/10.1016/0006-291x(88)90632-8).
- Pradhan, R., Dandawate, P., Vyas, A., Padhye, S., Biersack, B., Schobert, R., Sarkar, F.H., 2012. From body art to anticancer activities: perspectives on medicinal properties of henna. *Curr. Drug Targets* 13 (14), 1777–1798.
- Rabelo, A.C.S., Borghesi, J., Noratto, G.D., 2022. The role of dietary polyphenols in osteosarcoma: a possible clue about the molecular mechanisms involved in a process that is just in its infancy. *J. Food Biochem.* 46 (1), e14026.
- Rahman, M.M., Islam, M.R., Akash, S., Shohag, S., Ahmed, L., Supti, F.A., Rauf, A., Aljohani, A.S.M., Al Abdulmonem, W., Khaill, A.A., Sharma, R., Thiruvengadam, M., 2022. Naphthoquinones and derivatives as potential anticancer agents: an updated review. *Chem. Biol. Interact.* 368, 110198 <https://doi.org/10.1016/j.cbi.2022.110198>.
- Rasouliyan, F., Eskandani, M., Jaymand, M., Akbari Nakhjavani, S., Farahzadi, R., Vandghanoni, S., Eskandani, M., 2021. Preparation, physicochemical characterization, and anti-proliferative properties of Lawsone-loaded solid lipid nanoparticles. *Chem. Phys. Lipids* 239, 105123. <https://doi.org/10.1016/j.chemphyslip.2021.105123>.
- Roy, A., Ahuja, S., Bharadvaja, N., 2017. A review on medicinal plants against cancer. *J. Plant Sci. Agric. Res.* 2, 8.
- Shukla, B., Saxena, S., Usmani, S., Kushwaha, P., 2021. Phytochemistry and pharmacological studies of *Plumbago zeylanica* L.: a medicinal plant review. *Clin. Phytosci.* 7 (1), 34. <https://doi.org/10.1186/s40816-021-00271-7>.
- Tokarz, K.M., Makowski, W., Tokarz, B., Hanula, M., Sitek, E., Muszyńska, E., Jędrzejczyk, R., Banasiuk, R., Chajec, Ł., Mazur, S., 2020. Can ceylon leadwort (*Plumbago zeylanica* L.) acclimate to lead toxicity?—studies of photosynthetic apparatus efficiency. *Int. J. Mol. Sci.* 21 (5) <https://doi.org/10.3390/ijms21051866>.
- Vaseva, A.V., Moll, U.M., 2009. The mitochondrial p53 pathway. *Biochimica et Biophysica Acta (BBA) - Bioenergetics* 1787 (5), 414–420. <https://doi.org/10.1016/j.bbabi.2008.10.005>.
- Wan, G., Tao, J.-G., Wang, G.-D., Liu, S.-P., Zhao, H.-X., Liang, Q.-D., 2016. In vitro antitumor activity of the ethyl acetate extract of *Potentilla chinensis* in osteosarcoma cancer cells. *Mol. Med. Rep.* 14 (4), 3634–3640. <https://doi.org/10.3892/mmr.2016.5679>.
- Yan, L., Huang, H., Zhang, Y., Yuan, X., Yan, Z., Cao, C., Luo, X., 2020. Involvement of p53-dependent apoptosis signal in antitumor effect of Colchicine on human papilloma virus (HPV)-positive human cervical cancer cells. *Biosci. Rep.* 40 (3) (BSR20194065).
- Yang, K.M., Pyo, J.O., Kim, G.-Y., Yu, R., Han, I.S., Ju, S.A., Kim, W.H., Kim, B.-S., 2009. Capsaicin induces apoptosis by generating reactive oxygen species and disrupting mitochondrial transmembrane potential in human colon cancer cell lines. *Cell. Mol. Biol. Lett.* 14 (3), 497–510. <https://doi.org/10.2478/s11658-009-0016-2>.
- Zhang, S., Jiang, S., Deng, N., Zheng, B., Li, T., Liu, R.H., 2022. Phytochemical profiles, antioxidant activity and antiproliferative mechanism of *Rhodiola rosea* L. phenolic extract. *Nutrients* 14, 3602.
- Zhou, S., Wen, H., Li, H., 2019. Magnolol induces apoptosis in osteosarcoma cells via G0/G1 phase arrest and p53-mediated mitochondrial pathway. *J. Cell. Biochem.* 120 (10), 17067–17079. <https://doi.org/10.1002/jcb.28968>.
- Zhu, H., Chen, D., Xie, X., Li, Y., Fan, T., 2021. Melittin inhibits lung metastasis of human osteosarcoma: evidence of wnt/β-catenin signaling pathway participation. *Toxicol.* 198, 132–142. <https://doi.org/10.1016/j.toxicol.2021.04.024>.